ORIGINAL PAPER

A new ICP–TOFMS. Measurement and readout of mass spectra with 30 μs time resolution, applied to in-torch LA–ICP–MS

Martin Tanner · Detlef Günther

Abstract In-torch LA–ICP–MS was implemented into an in-house-built ICP–TOFMS system. The fast data acquisition capabilities of the new configuration allowed simultaneous multi-element measurement and readout of in-torch LA–ICP–MS signals with 30 μs time resolution. The measurements confirmed previously observed fine structures of in-torch generated signals and provided new insights in the dynamic processes in the plasma on a microsecond time scale. The new setup is described in detail and first figures of merit are given.

Keywords In-torch · Laser ablation · ICP–TOFMS · Brass · Microsecond resolution

Introduction

In-torch laser ablation sampling has already been successfully implemented in ICP–AES [1] and commercial ICP–MS systems with quadrupole-based mass filters (QMS) and with time-of-flight technology (TOFMS). Each of these approaches provided fundamental insights into the fast and intense in-torch generated signals. Using the ICP–QMS, a detailed study on the signal fine structure with time resolution of 20 μs but no simultaneous multi-element measurement was possible [2, 3]. First data on elemental and isotopic ratios of in-torch LA–ICP–MS signals have been acquired using a commercial ICP–TOFMS but the time resolution of 12.75 ms was insufficient for the time resolution requirements of such signals [4]. ICP–TOFMS

M. Tanner · D. Günther (✉)
Laboratory of Inorganic Chemistry, ETH Zurich,
8093 Zurich, Switzerland
e-mail: guenther@inorg.chem.ethz.ch

has already in the first publication been claimed to provide sub-ms time resolution [5]. Even though ion extraction and mass spectra acquisition have been possible at frequencies >10 kHz, the data could not be read out because of limitations of the electronic system. Until now commercially available ICP–TOFMS have provided mass spectra readout at rates of up to 78 spectra s^{-1} (GBC Optimass 9500, 50 spectra s^{-1}; Leco Renaissance, 78 spectra s^{-1}).

ICP–MS systems with static sector field (SF) mass analyzers, for example in Mattauch–Herzog geometry [6, 7], would be an ideal alternative to TOFMS for acquisition of fast transient multi-element signals. Unlike TOFMS, static SFMS has no restrictions in terms of duty cycle. However, detectors for simultaneous acquisition of full mass spectra are still in the stage of development [8].

Fully time resolved multi-element signal acquisition with microsecond time resolution offers prospects of new analytical applications for in-torch LA–ICP–MS and fundamental insights into the dynamic processes inside the plasma during introduction of sample aerosols.

The aim of this study was to measure in-torch generated laser ablation signals:

1. fully time resolved; and
2. with simultaneous multi-element detection.

Full time resolution is required for optimum S/N ratios and to study the dynamics of such signals. Simultaneous multi-element measurement is necessary for quantification of elements in unknown samples which would open the way for in-torch LA–ICP–MS into many fields of fundamental and applied sciences. The project involved the coupling of a TOFMS equipped with fast data readout to an ICP generator from a commercial ICP–QMS instrument. In-torch LA–ICP–MS was performed on this new configuration to determine first figures of merit and to describe the dynamic processes

of various ion species in the argon plasma during pulsed introduction of laser-generated aerosols.

Instrumentation and experimental

Figure 1 gives an overview of the instrumentation used for this project. The setup can be divided into three major parts, the laser ablation unit, the ICP, and the TOFMS. The following paragraphs describe these parts, their physical connection and the necessary triggering scheme for communication. Table 1 lists the instrument parameters used for the experiments.

Laser ablation

The same laser system as described in previous studies [2–4] was used. A 266 nm laser beam was focused on to the sample surface using a 5× objective (OFR, LMU-5X-266). The Q-switch trigger provided by the laser system was used to precisely start the data acquisition after each laser shot.

ICP

The ICP RF generator was taken from a commercial ICP–MS instrument (Perkin–Elmer Sciex, Elan 6000). The generator was operated independently from the original ICP–MS software via service software and an additional 5 V

power supply for the internal driver card. The torch box showed the modifications already described in Ref. [2] which allowed laser ablation sampling inside the torch. This setup allowed sample placement and exchange with running plasma by pulling the entire injector tube out, exchanging the sample, and pushing the sample back in position. Since the RF generator was removed from its original instrument a new carrier was constructed in house to hold the generator and adjust the vertical position of the torch relative to the interface. The horizontal position and the position of the sampler cone relative to the torch (sampling depth) were manually adjustable. Sampling depth was set to 10 mm as in the original Elan 6000 geometry. The gas flows were regulated via mass flow controllers (Perkin–Elmer Sciex, 247C). Argon was used as plasma, auxiliary, and carrier gas.

Water-cooled vacuum interface

A water cooled vacuum interface of an Elan 6000 ICP–MS was adapted to the TOFMS to couple the ICP to the TOFMS. The photon stop was not necessary for the TOFMS configuration, where the detector is not on axis with the ion flight path through the interface, and was therefore removed. Beside this, the geometry of the interface remained unchanged, including the slide valve behind the interface-skimmer cone. The vacuum interface was pumped by a rotary vane pump (Pfeiffer Vacuum, UNO 065 D) providing a pumping power of 65 $m^3 h^{-1}$.

TOFMS

The mass spectrometer coupled to the ICP was a TOFMS (Tofwerk, W-TOF), a compact instrument of 34×72×35 cm ($l×w×h$). It can be operated at high mass resolution (W-mode) or low mass resolution (V-mode). Since W-mode is higher in resolution but lower in sensitivity, the experiments were carried out in V-mode only. The detector is a combination of a micro channel plate (MCP) and a scintillator (Burle, BiPolar TOF detector) which allows higher sensitivity and an extended dynamic range compared to MCP only.

The ion beam from interface-sampler and interface-skimmer cones was sampled into the TOFMS by the TOF-sampler cone (stainless steel, 3 mm i.d.). Due to the gate valve, the distance between interface-skimmer and TOF-sampler was about 33 mm. The vacuum for the MS was originally generated by a 3-stage turbomolecular pump (Pfeiffer Vacuum, TMH 261-250-005) with volume flow rates of 280, 205 and 5 L s^{-1}. This pumping power was designed for low-pressure ion source applications such as glow discharge (GD) (e.g. 0.75 mbar Ar) [9]. Due to the expected higher gas load of the ICP source (atmospheric pressure), the 5 L s^{-1} stage was disconnected and an
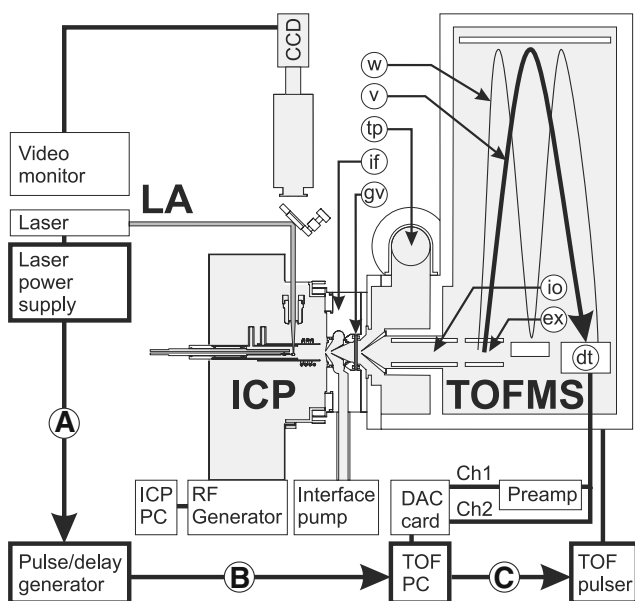

Fig. 1 Overview of the new ICP–TOFMS setup. Abbreviated system components, explanations are given in the text: (*w*) ion flight path in W-mode, (*v*) ion flight path in V-mode, (*tp*) additional turbo pump pumping the volume after the skimmer cone to $2×10^{-3}$ mbar, (*if*) water cooled interface, (*gv*) gate valve, (*io*) ion optics, $1×10^{-4}$ mbar, (*ex*) ion extraction zone, (*dt*) detector, $2×10^{-6}$ mbar

Table 1 Summary of ICP–TOFMS and laser ablation operating conditions

Parameter	Setting	Parameter	Setting	
ICP	Elan 6000	Laser	Brilliant Nd:YAG	
ICP power (W)	1300	Laser λ (nm)	266	
Gas	Ar	Crater diameter (μm)	50–80	
Plasma gas (L min^{-1})	15	Laser energy (mJ)	0.4–2[a]	
Aux. gas (L min^{-1})	1	Laser frequency (Hz)	2	
Carrier gas (L min^{-1})	1.1			
TOF power supply	(V)	Data acquisition	Acquiris, AP240	
Skimmer	500		Ch$_1$	Ch$_2$
Lens	1,300	Preamplification	100×	1×
Postacceleration	3,800	Full-scale (V)	2	0.5
Deflector	−45	Resolution (bin_S)	256	256
Deflector flange	−41	bin_S-size (mV)	7.81	1.95
Ion extractor	−95	Offset (mV)	−66	20.2
U-low	630	Threshold recording		
U-high	85	Threshold (bin_S)	12	0
U+low	39	Baseline (bin_S)	7	0
U+high	670			
Reflector backplane	675	Single ion (mV ns)		1.8
Reflector grid	970			
Hardmirror	0	f_{TOF} ($= 1/T_{TOF}$) (kHz)		33⅓
Ion Lens 1	−48	Extr. pulse height (V)		2,000
Ion Lens 2	−110	Extr. pulse width (μs)		2
Micro channel plate	800	Averaged wf per segment		1–10
Scintillator	2,800	Segments per block		50–120
Photomultiplier	640	Blocks per write		200

[a] Laser energy was measured before focusing objective

additional turbomolecular pump installed (BOC Edwards, EXT 250 Hi) with a volume flow rate of 210 L s^{-1}. The vacuum with ICP running and open gate valve was 2×10^{-3} mbar in front of the TOF-sampler, 1×10^{-4} mbar at the TOF extraction, and 2×10^{-6} mbar at the detector.

Data acquisition

The sampling rate of the data acquisition card (Acquiris, AP240) can be chosen between 1 and 2 gigasamples per second (Gsample s^{-1}). For the current study 1 Gsample s^{-1} was chosen. After each TOF extraction one time-dependent signal (waveform) was acquired. Several waveforms could be combined into segments before data readout from the data acquisition (DAQ) card memory to the TOFPC. For the current experiments the time between TOF extractions (T_{TOF}) was set to 30 μs (TOF frequency, f_{TOF}=33⅓ kHz) and waveforms of 27 μs were acquired covering the m/z range up to 280 with 27,000 data points.

The intensity of the signal from the detector was sampled by the two channels, Ch1 and Ch2, of the DAQ card with 256 bit (32 byte) resolution, thus dividing the full scale per channel into 256 signal bins, bin_S. The dynamic range of a single waveform using the parameter settings given in Table 1 covered the range from the threshold of 0.39 mV to 19.45 mV (Ch1 100× preamplified) and subsequently to 520 mV (Ch2). The dynamic range of an averaged mass spectrum depends furthermore on the number of integrated waveforms.
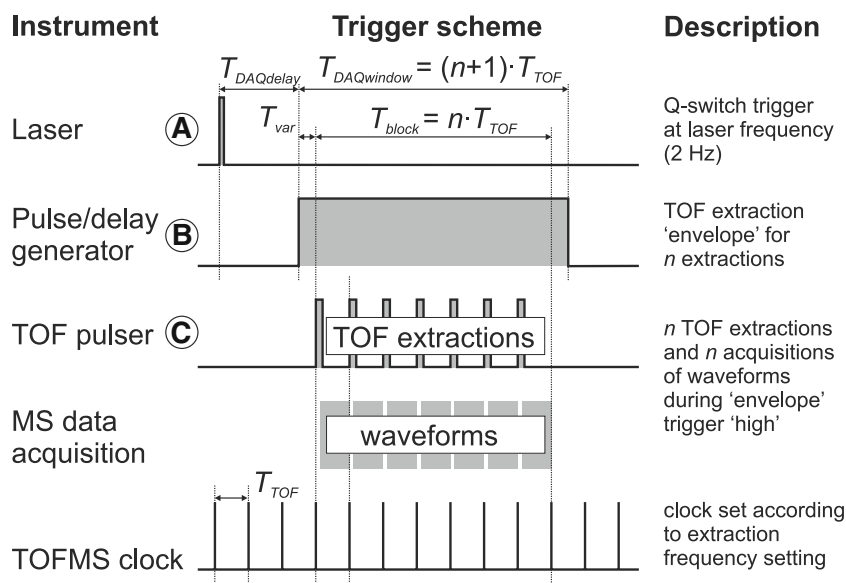
One waveform or segment consists of 27,000 signal data points or 864 kilobytes of data. The DAQ card memory capacity of 256 megabytes (MB) thus allowed acquisition of 148 waveforms or segments per data block into the two DAQ channels before data readout to the TOFPC. If the signal of each of the 200 laser pulses was recorded with maximum number of segments (256 MB on the DAQ card memory) a total file size (the signals of Ch1 and Ch2 combined to one signal) of >25 gigabytes resulted.

With f_{TOF}=33⅓ kHz at full time resolution (one segment = one waveform) about 4.5 ms of signal was recordable before data download. Since data download required about 300 ms the maximum laser frequency was 2 Hz.

Triggering

Figure 2 shows an overview of the different triggers used for communication between laser and TOFMS system. In the schematic overview of the instrumentation (Fig. 1) the corresponding communication chain between the involved instruments is drawn by arrows indicating sender and receiver of a trigger signal. Q-switch trigger (A) was sent from the laser power supply to the digital delay/pulse generator (Oxford Research Systems, DG 535). The delay/pulse generator sends a trigger (B) to the TOFPC according

Fig. 2 Scheme of the triggers used to establish communication between laser and TOFMS

In the current setup, laser and MS followed different internal clocks which were left to run independently. The laser was running at its internal flash lamp frequency of 20 Hz assuring stable output power. T_{TOF} could be set for each individual experiment. The acquisition of a block of waveforms always started at the beginning of the next TOF period after trigger (B) went "high". This left an uncertainty (T_{var}) of 30 μs (one T_{TOF} period) between laser pulse and data acquisition. $T_{DAQwindow}$ was accordingly set to $(n+1)\times T_{TOF}$. T_{var} was of the order of 1% of $T_{DAQdelay}$ or 10 % of
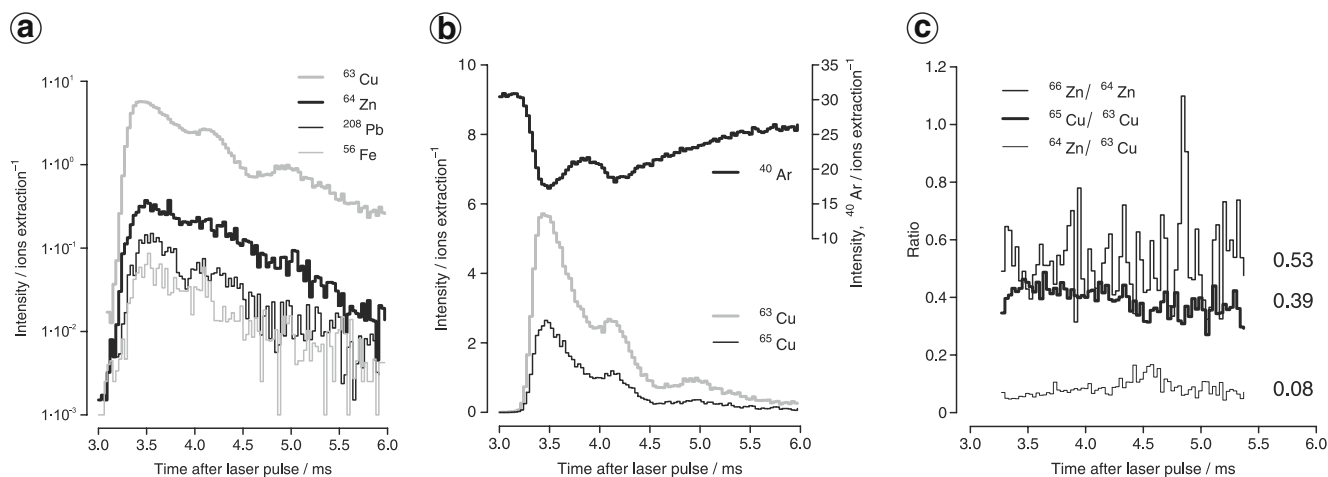
to the requirements of the data-acquisition software. This "envelope" pulse of length $T_{DAQwindow}$ defined the time window during which TOF extractions and data acquisition occurred. For the in-torch LA experiments the delay time between laser pulse and data acquisition ($T_{DAQdelay}$) was set to start TOF extractions at the beginning of the signal (2–3 ms after the laser pulse). As soon as trigger (B) went "high" a predefined block of n TOF extractions and waveform acquisitions started (T_{block}), which is indicated by the trigger sequence (C).

Fig. 3 (**a**) Averaged time-dependent profiles of 200 laser pulses from brass on a log scale (corresponding to the mass spectrum given in Fig. 6). The time-dependent signals of Cu and Zn show the same general trend but the fine structure is more pronounced for Cu than for Zn, indicating different sampling and/or excitation in the plasma. (**b**) Transient signals of ^{63}Cu, ^{65}Cu, and ^{40}Ar on a linear scale. The patterns of the two Cu isotopes show the same fine structure and represent their relative abundance. ^{40}Ar, the main species in the argon plasma, shows a transient signal with a pattern opposite to the analyte ions, indicating a temperature drop of the plasma depending on the aerosol concentration in the plasma. (**c**) Ratios of Zn and Cu isotopes and between the two elements

Table 2 Element concentrations of the brass standard SRM MBH 31X B26 according to the values given in the certificate

Element	wt %	Element	wt %	Element	wt %	Element	wt %
Sn	1.49	Ni	1.51	Cu	62.9	P	0.019
Pb	1.02	Al	1.01	As	0.071	S	<0.005
Zn	(30)	Si	0.27	Bi	0.11(7)		
Fe	1.07	Mn	0.50	Sb	0.069		

the duration of the observed first signal peak (Fig. 3) and was neglected in this study.

Samples

The laser ablation study was carried out using a metal standard reference material. The SRM MBH B26 is a brass standard with a Zn:Cu ratio of ~1:2. The certified element concentrations are given in Table 2.

Results

Mass spectrum of the gas blank

Figure 4 shows a mass spectrum of the gas blank. This spectrum is the average of 24,000 waveforms which corresponds to a total acquisition time of 720 ms. The species $^{14}N^+$, $^{16}O^+$, $^1H_2\ ^{16}O^+$, $^{40}Ar^{2+}$, $^{36,38,40}Ar^+$, and $^{40}Ar_2^+$, were identified.

Mass spectrum of the brass standard

Figure 5 shows a mass spectrum after in-torch laser ablation of the brass standard material. The spectrum corresponds to a total number of 20,000 averaged spectra acquired in 200 blocks, each starting 3 ms after a laser pulse (one waveform/segment, 100 segments/block, 200 blocks, total analysis time=100 s). All major isotopes of the certified elements were identified except for arsenic, sulfur, and

phosphorus. ^{58}Fe was isobarically overlapped by ^{58}Ni and $^{29,30}Si$, ^{57}Fe, ^{61}Ni, ^{70}Zn, and ^{75}As were within the spectral noise. The least abundant tin isotopes, ^{112}Sn (0.97%), ^{114}Sn (0.66%), ^{115}Sn (0.34%), and the isotopes of antimony, ^{121}Sb (57.2%) and ^{123}Sb (42.8%), were close to the spectral noise level.

Mass resolution

Figures 6(a) and (b) give an illustration of the mass resolution achieved with the current ICP–TOFMS instrument. The resolving power ($m/\Delta m$) was calculated on the 10% peak-height criterion. The margins were interpolated from the signal data points above and below 10%. The mass resolution for ^{40}Ar and ^{208}Pb was calculated to be 680 and 1,300, respectively.

Abundance sensitivity

The abundance sensitivity of an MS instrument describes how much of the tail of a certain signal peak contributes to the BG level at neighboring m/z. To calculate the abundance sensitivity of the current setup the signal peak of $^{40}Ar^+$ was chosen because it was the only signal with sufficient intensity to calculate abundance sensitivity on the low (AS^{-1}) and high (AS^{+1}) mass sides. The signal given in Fig. 6(c) shows no signal peaks of specific isotopes apparent on m/z=39 and 41. It is therefore assumed that the entire signal in the m/z range from ~38.5 (high mass side of the $^{38}Ar^+$ peak) to ~53.5 (low mass side of $^{54}Fe^+$)
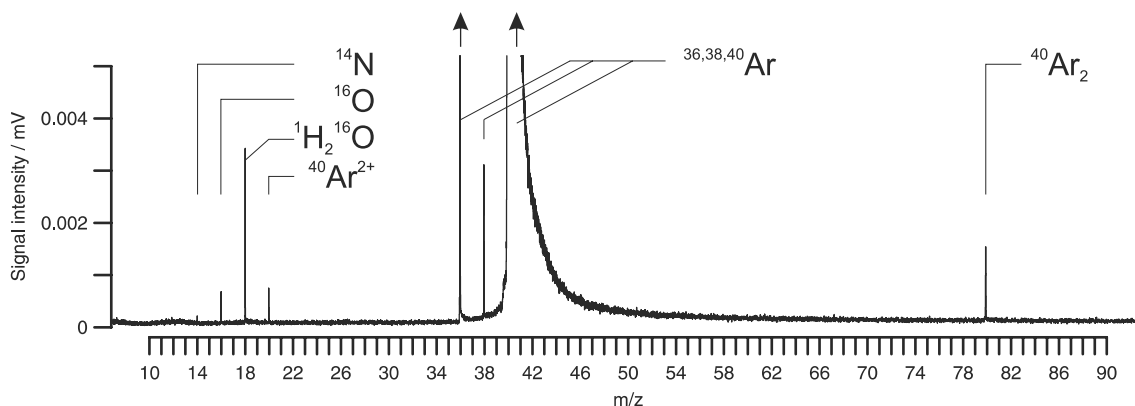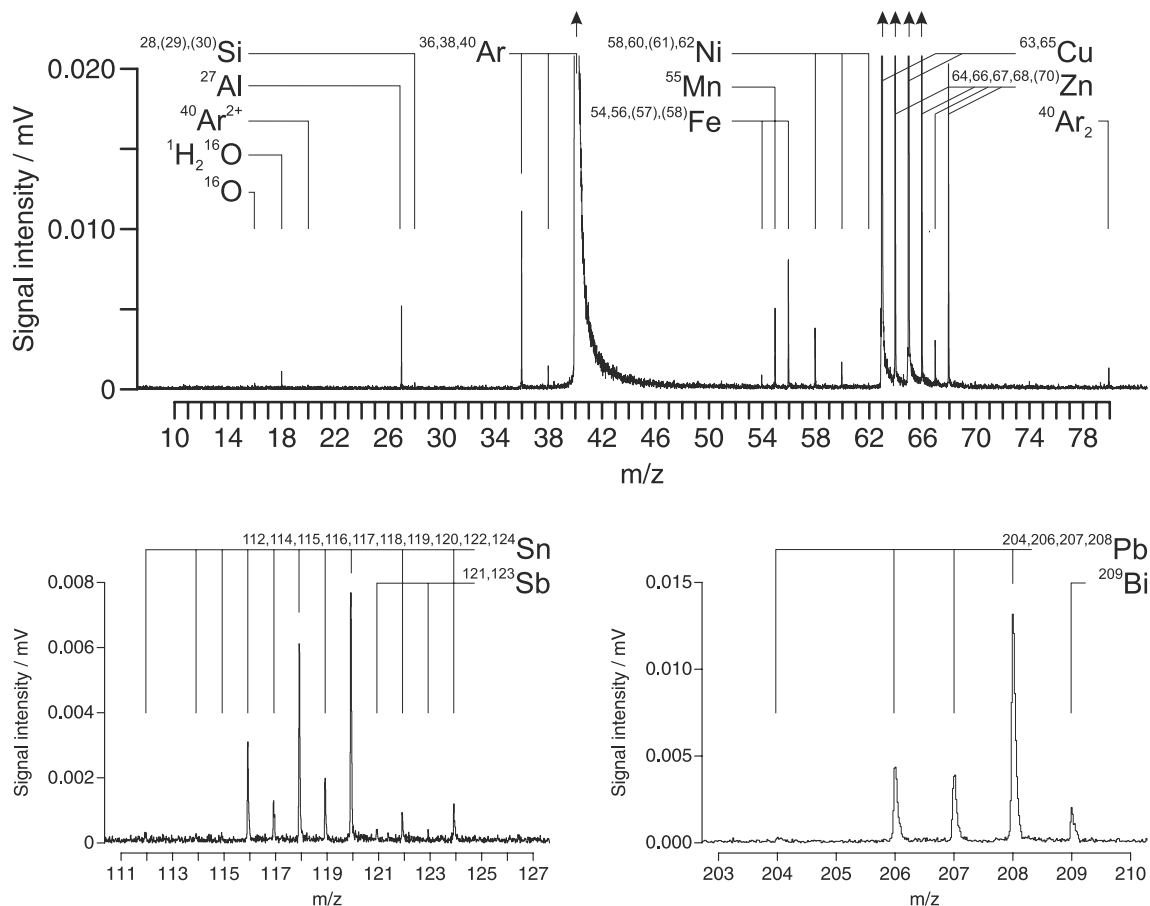

Fig. 4 Blank spectrum after 720 ms acquisition time

Fig. 5 Mass spectrum of brass after 200 laser pulses (100 s total analysis time). T_{TOF}=30 μs, 3 ms integration time per laser pulse, 600 ms total integration time

depends on $^{40}Ar^+$ only. Net background (*netBG*) was calculated from the average signal in the *m/z*-ranges=35± 0.5 (S_{35}), 39±0.5 (S_{39}) and 41±0.5 (S_{41}). S_{35} was assumed not to be influenced by the argon signal and to be close enough to *m/z*=40 to estimate the zero level of all three mass ranges. The net BG values are calculated using Eqs. 1 and 2:

$$netBG_{39} = S_{39} - S_{35} \tag{1}$$

$$netBG_{41} = S_{41} - S_{35} \tag{2}$$

The abundance sensitivity was derived by calculations according to Eqs. 3 and 4

$$AS^{-1} = \frac{netBG_{39}}{S_{40}} \tag{3}$$

$$AS^{+1} = \frac{netBG_{41}}{S_{40}} \tag{4}$$

with S_{40} the signal maximum measured for $^{40}Ar^+$. From the values given in Fig. 6(c) can be calculated: $AS^{-1}=1\times10^{-5}$

and $AS^{+1}=5\times10^{-4}$. For the Leco Renaissance instrument no values of abundance sensitivity have been given in the literature and only Emteborg et al. have mentioned an AS^{-1} value of 10^{-5} reported by the manufacturer [10]. This number has apparently been based on investigations on a prototype of the Renaissance instrument where the reciprocal value of AS^{-1} was determined to be "at least in the 10^6 range" and no value has been given for AS^{+1} [11]. The GBC, Optimass 8100 was described with $AS^{-1}=3\times10^{-6}$ and $AS^{+1}=7\times10^{-5}$ [12]. However, for attenuation of the high-mass side of the investigated signal peak a "blanker system" was used. QMS systems usually perform with $AS^{-1}<10^{-6}$ and $AS^{+1}<10^{-7}$ [13].

From mV to the number of ions

The gray peak areas given in Figs. 6(a) and (b) represent the signal integrals used by the software to calculate time-dependent signal intensities. The borders of these areas can be set in the software as mass resolution values. A value of 900 was used for all mass peaks. The number of counted ions per TOF extraction (ions extraction^{-1}) was calculated by division of the signal integrals (in mV ns) by the single
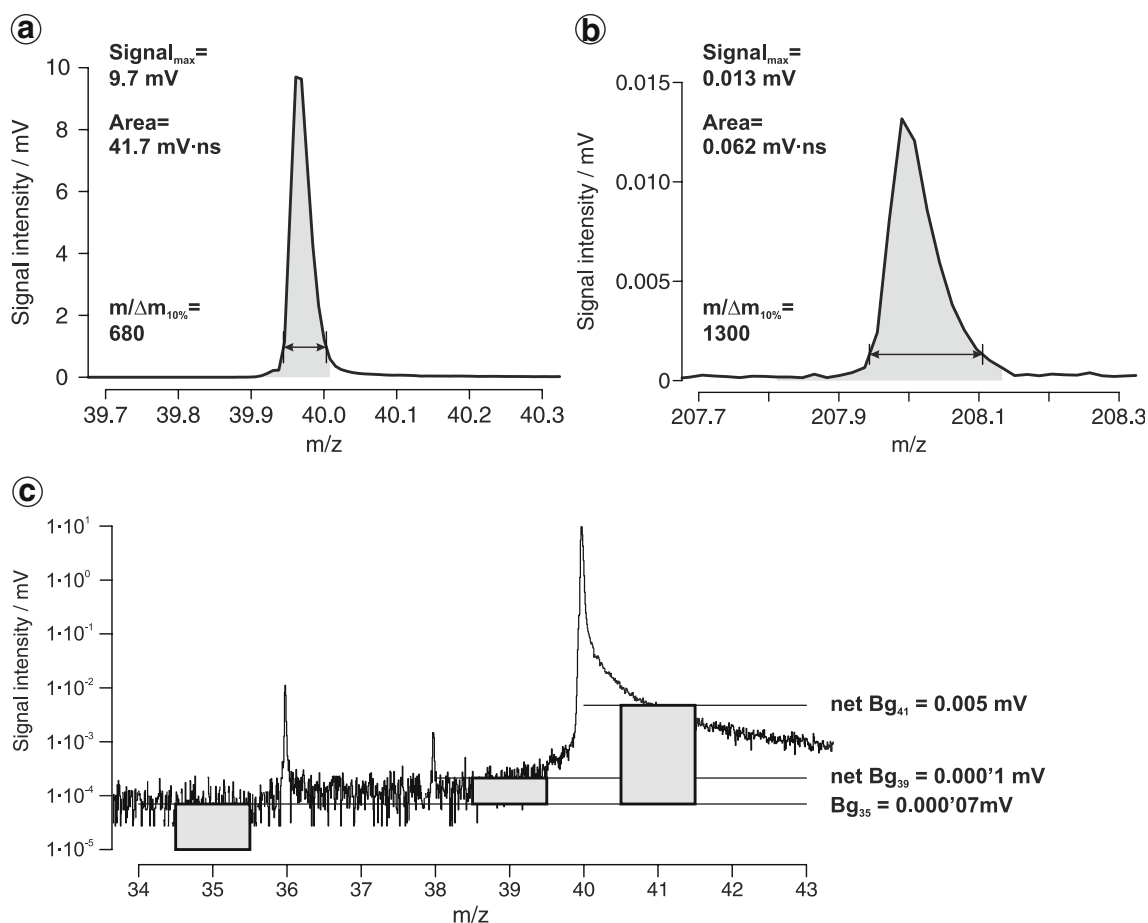
Fig. 6 Details of the mass spectrum of brass (Fig. 5). (**a**) and (**b**) show the mass peaks of ^{40}Ar and ^{208}Pb. The *arrows* represent the mass range at 10% of peak maximum used for calculation of the mass resolution. *Gray areas* represent the integrals of the peaks used for calculation of element-specific transient signals. The margins of the integrals were set as software parameters and correspond to a mass resolution of 900. (**c**) Mass spectrum in the m/z range 34–43 on a log scale with *gray areas* indicating range and average intensities of background values used for calculation of the abundance sensitivity

ion value (mV ns). The signal integral of single-ion events was measured with the extraction pulse voltage set to zero, thus reducing the ion beam at the detector to a series of discrete events. A typical single-ion event was calculated as average value of a few thousands of such events to be of 1.8 mV ns. The signal integrals for ^{40}Ar and ^{208}Pb were 41.8 and 0.062 mV ns and translate to 32 and 0.05 ions extraction^{-1}, respectively. This means that an average number of $100 \times 0.05 = 5$ counts of ^{208}Pb was detected within a time period of 3 ms after each laser shot and that the ^{208}Pb peak given in Fig. 6(b) corresponds to a total number of $200 \times 5 = 1,000$ counted ions.

Time dependent signals

Figure 3 shows the first multi-element transient signals measured at 30 μs time resolution. These transients represent the temporal behavior of the peak integrals of the mass spectrum given in Fig. 5. Each data point represents the average of 200 integrated mass peaks measured at

a given time after the laser pulse; 100 data points with time differences of 30 μs sum up to 3 ms of transient multi-element signal.

The signal of the two Cu isotopes in Fig. 3(b) shows the same double peak signal shape as described for the La and Cs isotopes for in-torch LA–ICP–QMS with 20 μs resolution. A connection of the signal structure with the aerosol formation process has been assumed [3]. Similar multi-peak signals have been observed by Gurevich et al. from a novel laminar flow ablation cell and ablating a brass sample using a fs-laser and 0.02 mJ pulse^{-1} laser energy. They have ascribed the observed multi-peak pattern to the formation of vortices within the aerosol clouds [14]. Koch et al. have investigated formation of the aerosol cloud using a high-speed camera and developed a model for ablation under He and Ar atmospheres [15]. The aerosol cloud calculated for an Ar atmosphere 1 ms after laser pulse shows a radius of ~6 mm. This corresponds well to the aerosol residence time in the plasma and the time difference of the first two peaks observed by Tanner and Günther [3]. An alternative

explanation of the smooth pattern of the observed signal fine structure in the averaged single-shot signals could be related to dynamic plasma effects caused by the pulsed introduction of dense aerosol fractions. Fey et al. have studied the optical emission of the Ar(6d) line which appeared as damped sinusoidal waves of ~1 kHz frequency appearing 2 ms after pulsed interruption of an ICP. From the dependency of the wave frequency on the observation distance above load coil they have concluded, that these waves travel through the plasma and have their origin in the plasma expansion zone [16]. The pattern of in-torch-generated signals could thus be interpreted as superposition of a sinusoidal wave caused by the shock wave of the laser pulse and a single, in-cell generated laser ablation signal (sharp rise and exponential decay) of reduced duration.

The time-dependent ^{40}Ar-signal shows a pattern opposite to the main matrix element Cu with a start value of 30 ions extraction^{-1}, a sharp signal drop of >1/3 of the initial value and slow signal recovery parallel to the decrease of the signals of the analyte isotopes. This observation corresponds well to the data published by Stewart et al. for the behavior of the plasma after introduction of single droplets of defined size and element concentration. They have explained the drop in the ^{40}Ar-signal by reduced ionization in the plasma which is cooled through dissolvation of the droplets [17]. Hence, the same effect was observed here to result after vaporization of laser-generated solid aerosol particles. Leach et al. have recorded the time-dependent signals of plasma matrix ions ($^{14}N^+$, $^{36}Ar^+$, $^{40}Ar^{2+}$) during single laser-shot events using an ICP–TOFMS and observed a direct, inverse relationship between these ions and the analyte ions, depending on the amount of ablated material [18].

Ratios

Even though the patterns of the isotopes of an element show the same temporal development (e.g. ^{63}Cu and ^{65}Cu in Fig. 3(b)), the patterns between elements show differences, as shown for ^{64}Zn and ^{63}Cu in Fig. 3(a). The transient ratios of $^{65}Cu/^{63}Cu$ (expected value=0.44), $^{66}Zn/^{64}Zn$ (expected value=0.57) and $^{64}Zn/^{63}Cu$ are given in Fig. 3(c). The isotopic ratios found were 11 and 7% lower than the expected values with the heavier isotopes reduced relative to the lighter ones. Therefore this observation cannot be

connected to mass bias where the lighter ions are discriminated relative to the heavier ones. However, Myers measured lead in solution using a Leco Renaissance ICP–TOFMS for the ratios of $^{204}Pb/^{206}Pb$ and $^{207}Pb/^{206}Pb$ and found a mass bias favoring the lighter isotopes [19]. The Renaissance ICP–TOFMS did not have a linear response in the analog mode and the isotope ratios depended on the detector voltage and on the element concentration [20]. Transient signals measured with a GC coupled to ICP multicollector MS of about 1-2 s duration showed drifts in the isotopic ratios of mercury during the signal duration which did not show trends only related to mass and thus could not be explained by conventional mass-bias models [21]. More experiments are therefore needed to further evaluate the isotope ratio measurements with the current instrument and to distinguish between instrument-caused variation from the certified values or whether the observed mass bias can be related to the short intense mass load effecting the plasma.

For conventional in-cell LA–ICP-QMS it has been shown that the Zn/Cu ratios of the signals are related to the different particle-size fractions of the aerosol with Zn, the more volatile element, being enriched in the smaller particles and Cu found more in the bigger particles. Furthermore, Zn/Cu ratios have been reported to depend on the laser and gas parameters used for measurement but have always been found to be approximately 0.4–0.5 [22]. The value of 0.08 in our experiments indicates that a substantial part of the Zn-rich aerosol fraction of small particles is lost in the ICP, the interface, or in the TOFMS.

Instrument sensitivity

The sensitivity of the instrument for the elements given in Fig. 3(a) is listed in Table 3. I_{mean} is the average signal intensity found for a single laser shot. This number corresponds to the integrated peak of the average mass spectrum (e.g. Fig. 6) divided by the single ion value. I_{Int} is the integral of an averaged signal given in Fig. 3(a). Since for the signal a total number of 100 waveforms were averaged, this value is $100 \times I_{mean}$. The maximum intensity of the averaged signals (I_{max}) occurred ~3.5 ms after the laser pulse. In order to allow a general comparison with intensities of other DAQ settings or other instruments, the signal maxima were standardized (I_{maxStd}) to counts per second (cps).

Table 3 Instrument sensitivity

Element	Isotope	I_{mean} (ions extr. $^{-1}$)	I_{Int} (ions pulse^{-1})	I_{max} (ions extr. $^{-1}$)	I_{maxStd} (cps)	S (cps (µg g^{-1})$^{-1}$)
Copper	^{63}Cu	1.6	160	5.8	190,000	0.31
Zinc	^{64}Zn	0.12	12	0.38	13,000	0.043
Lead	^{208}Pb	0.035	3.5	0.16	5,200	0.50
Iron	^{56}Fe	0.017	1.7	0.085	2,800	0.27

Finally, sensitivity (S) was calculated for four elements and given in cps $(\mu g\ g^{-1})^{-1}$ using the concentrations of the elements given in Table 2.

To compare the instrument sensitivity with conventional in-cell systems, an approximation has to be done to translate in-torch signal intensities to in-cell signals. A conventional in-cell configuration with the same detection efficiency (ions per ablated atom) and a laser repetition rate of 10 Hz would generate an average transient ^{63}Cu signal of 1,600 cps, which results in a sensitivity of 0.0025 cps $(\mu g\ g^{-1})^{-1}$ copper in the analyzed brass standard sample. Pisonero et al. reported for analysis of the same brass standard, using a 266 nm laser with 10 J cm^{-2} and 1 L s^{-1} He as cell gas, an average Cu sensitivity of 660 cps $(\mu g\ g^{-1})^{-1}$ for 600 laser pulses in single-spot ablation [23]. The in house built ICP–TOFMS can therefore be assumed to provide about five orders of magnitude less detection efficiency compared to a conventional ICP-QMS. In the current measurements an average ion current of ~40 ions extraction^{-1} was measured. Since the ion optics, including the TOF sampler cone, were not optimized for an ICP configuration, a substantial improvement can be expected thorough redesign. The ion extraction zone in the TOFMS was designed for ion packages of up to 2,000 ions and factors of >50 in improvement through optimized ion optics would be limited by this extraction capacity. Further gain could only be realized by reduction of the Ar$^+$ ion concentration in the ion beam, which has been realized for ICP–QMS systems through additional collision or reaction cells [24, 25]. Implementation of a reaction/collision cell would also lead to improved cooling of the ions and eventually reduce the high abundance sensitivity. In-torch signals of ^{63}Cu already show an average of six ions extraction^{-1} at the maximum of a laser signal peak, and thus these signals allow 2–3 orders of magnitude improvement before copper ions alone would saturate the extraction zone.

Conclusions

A TOFMS with fast data readout was successfully combined with an ICP ion source. Simultaneous multi-element signals with time resolution of 30 μs were read out and investigated.

The mass resolution of the system was superior to that of ICP–QMS systems but the abundance sensitivity was higher, especially on the high-mass side. The in-torch LA–ICP–TOFMS system provided average ^{63}Cu signals from an analyzed brass standard corresponding to ~160 counted ions per laser pulse. The instrument detection efficiency was estimated to be five orders of magnitude lower than conventional ICP–QMS systems.

Maximum time resolution of 30 μs allowed first fully resolved acquisition and readout of in-torch LA–ICP–TOFMS signals. The sensitivity for zinc was very low

compared to the other measured elements, which indicates that a significant amount of the small particle fraction of the laser aerosol was lost during analysis. The Zn/Cu ratio in the different particle size fractions has been reported to be very sensitive to the chosen gas environment (He or Ar). Especially when using 266 nm laser ablation in argon, the LA–ICP–MS signal ratio has been reported to show a significant depletion in zinc [22]. However, it needs to be further evaluated, to what extent the Zn/Cu ratio for in-torch ablation can be optimized in terms of x/y position of the torch relative to the interface or in terms of the gas flows and the type of gas.

It has been shown that multi-element measurement in microsecond time resolution is possible using an in-house-built ICP–TOFMS. However, there is still limitation in the dynamic range compared to ICP–QMS systems that needs to be solved on the way to a fast, simultaneously measuring, and sensitive ICP–TOFMS. The advantages and future perspectives of such an instrument could clearly be demonstrated.

The development of simultaneous multi-element measurement capabilities with time resolution below 1 ms is of benefit for all applications where fast transient signals need to be measured, for example analysis of any very small object or single-shot analysis using LA–ICP–MS [26].

References

1. Liu XR, Horlick G (1995) Spectrochim Acta B 50:537–548
2. Tanner M, Günther D (2005) J Anal At Spectrom 20:987–989
3. Tanner M, Günther D (2007) J Anal At Spectrom 22:1189–1192
4. Tanner M, Günther D (2006) J Anal At Spectrom 21:941–947
5. Myers DP, Yang GLP, Hieftje GM (1994) J Am Soc Mass Spectrom 5:1008–1016
6. Burgoyne TW, Hieftje GM, Hites RA (1997) J Am Soc Mass Spectrom 8:307–318
7. Cromwell EF, Arrowsmith P (1996) J Am Soc Mass Spectrom 7:458–466
8. Barnes JH, Schilling GD, Hieftje GM, Sperline RP, Denton MB, Barinaga CJ, Koppenaal DW (2004) J Am Soc Mass Spectrom 15:769–776
9. Fliegel D, Günther D (2006) Spectrochim Acta B 61:841–849
10. Emteborg H, Tian XD, Adams FC (1999) J Anal At Spectrom 14:1567–1572
11. Myers DP, Li G, Mahoney PP, Hieftje GM (1995) J Am Soc Mass Spectrom 6:411–420
12. Sturgeon RE, Lam JWH, Saint A (2000) J Anal At Spectrom 15:607–616
13. Montaser A, Mclean JA, Huiying L, Mermet JM (1998) An introduction to ICP spectrometries for elemental analysis. In: Montaser A (ed) Inductively coupled plasma mass spectrometry. Wiley–VCH, New York

14. Gurevich EL, Hergenröder R (2007) J Anal At Spectrom 22:1043–1050
15. Koch J, Schlamp S, Rosgen T, Fliegel D, Günther D (2007) Spectrochim Acta B 62:20–29
16. Fey FHAG, Stoffels WW, Vandermullen JAM, Vandersijde B, Schram DC (1991) Spectrochim Acta B 46:885–900
17. Stewart II, Olesik JW (1999) J Am Soc Mass Spectrom 10:159–174
18. Leach AM, Hieftje GM (2000) J Anal At Spectrom 15:1121–1124
19. Myers DP, Mahoney PP, Li G, Hieftje GM (1995) J Am Soc Mass Spectrom 6:920–927
20. Emteborg H, Tian XD, Ostermann M, Berglund M, Adams FC (2000) J Anal At Spectrom 15:239–246
21. Krupp EA, Donard OFX (2005) Int J Mass Spectrom 242:233–242
22. Kuhn HR, Günther D (2003) Anal Chem 75:747–753
23. Pisonero J, Fliegel D, Günther D (2006) J Anal At Spectrom 21:922–931
24. Hattendorf B, Günther D (2000) J Anal At Spectrom 15:1125–1131
25. Rowan JT, Houk RS (1989) Appl Spectrosc 43:976–980
26. Durrant SF, Ward NI (2005) J Anal At Spectrom 20:821–829